Supplementary Information

Effect of an Electrolyte Cation on Detecting DNA Damage with the Latch Constriction of α-Hemolysin

Robert P. Johnson, Aaron M. Fleming, Cynthia J. Burrows*, Henry S. White*

*burrows@chem.utah.edu, *white@chem.utah.edu

Department of Chemistry, University of Utah, 315 South 1400 East, Salt Lake City, Utah, 84112-0850.

List of Contents

1. Translocation of a dC_{60} homopolymer in 1.00 M NEt_4Cl

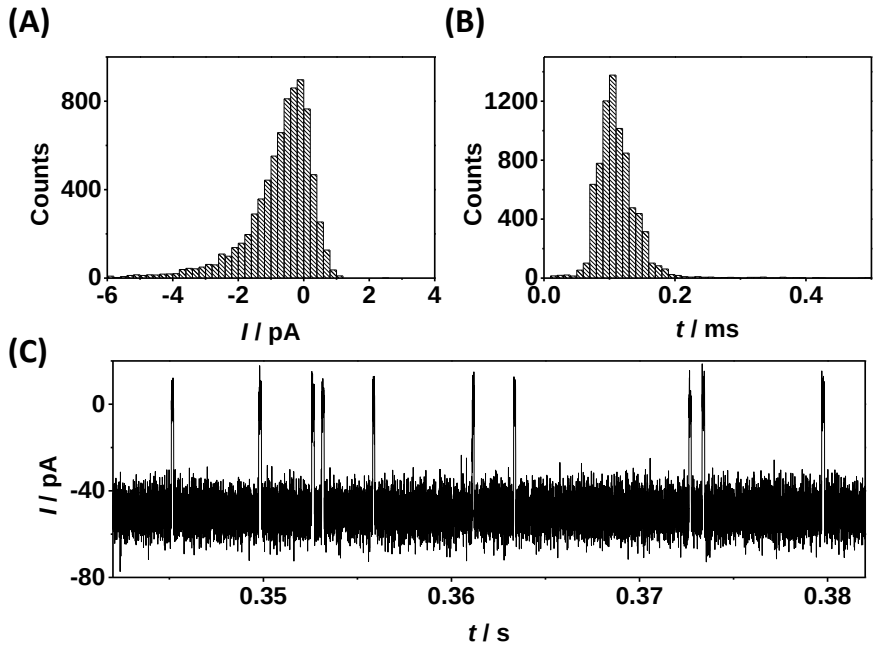

Figure. S1. Translocation of a dC_{60} homo-polymer through αHL in 1.00 M NEt_4Cl electrolyte. (A) Current and (B) time histograms of the translocation events. (C) Representative current-time trace. Data were recorded at an applied bias of 120 mV in a 10 mM phosphate buffer (pH 7.5). Data were collected at 500 kHz and filtered at 100 kHz. Counts indicate the number of ssDNA translocation events.

2. The effect of electrolyte anion on detecting a furan with the latch constriction of α-hemolysin

Intrigued by the strong dependence of the difference in the blockage current on cation choice, we briefly extended our study to the effect of anion in detecting a furan site at the latch constriction (Fig. S2). The open channel current in a mixed 0.95 M KNO_3/0.05 M KCl electrolyte is 12% smaller relative to a 1 M KCl electrolyte because the NO_3^- anion is less mobile. In this electrolyte, the majority of the current is carried by the K^+ and NO_3^- ions; a small amount of Cl^- is required to maintain the potentials of the two Ag/AgCl electrodes on either side of the nanopore. Despite an ~15 pA decrease in I_0, changing the anion from Cl^- to NO_3^- has a very limited effect on the measured current during dsDNA residence in the pore (~1 pA) and no effect on ΔI_T (1.6 ± 0.2 pA for 1 M KCl and 1.6 ± 0.1 pA for 0.95 M KNO_3/0.05 M KCl) for duplexes 9F and 13F. The presence of the highly negatively charged dsDNA inside the pore acts to reverse the selectivity of the protein channel (αHL by itself is weakly anion selective [1]), and anions are largely excluded from the pore when DNA is present. While both cations and anions contribute to the open channel current, cations dominate the conductivity of the pore when dsDNA resides in the αHL channel. Significant anion exclusion from the pore during ssDNA translocation has previously been predicted; [2-6] the increased charge density of dsDNA compared to ssDNA is expected to increase this exclusion effect.

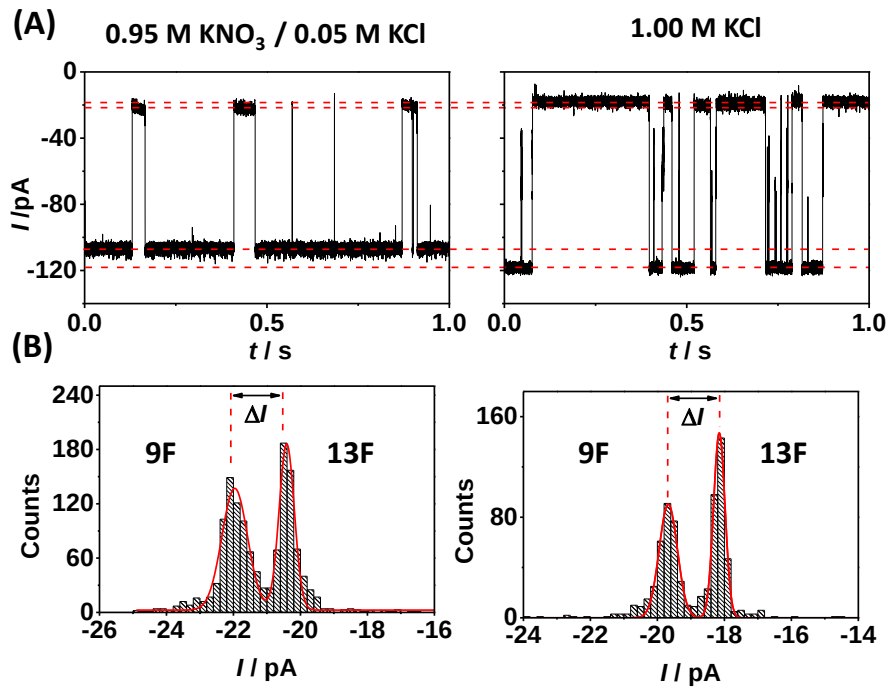

Figure S2. Effect of anion on the open channel and dsDNA blockage current in changing from a 1.00 M KCl to a 0.95 M KNO_3/0.05 M KCl electrolyte. (A) Current-time traces show a 12% decrease in open channel current, and small increase in current during dsDNA residence. (B) Current histograms showing no effect of the anion on the measured current difference between duplexes 9F and 13F during residence inside the pore. Experiments were carried out in 10 mM phosphate buffer (pH 7.5) at 25 °C with electrolyte added as indicated. Data were collected at 500kHz and filtered at 10kHz. Counts indicate the number of dsDNA unzipping events.

3. Unzipping times and melting temperatures (T_m) values for each duplex as a function of cation as an accompaniment to Figure 4 in the main text

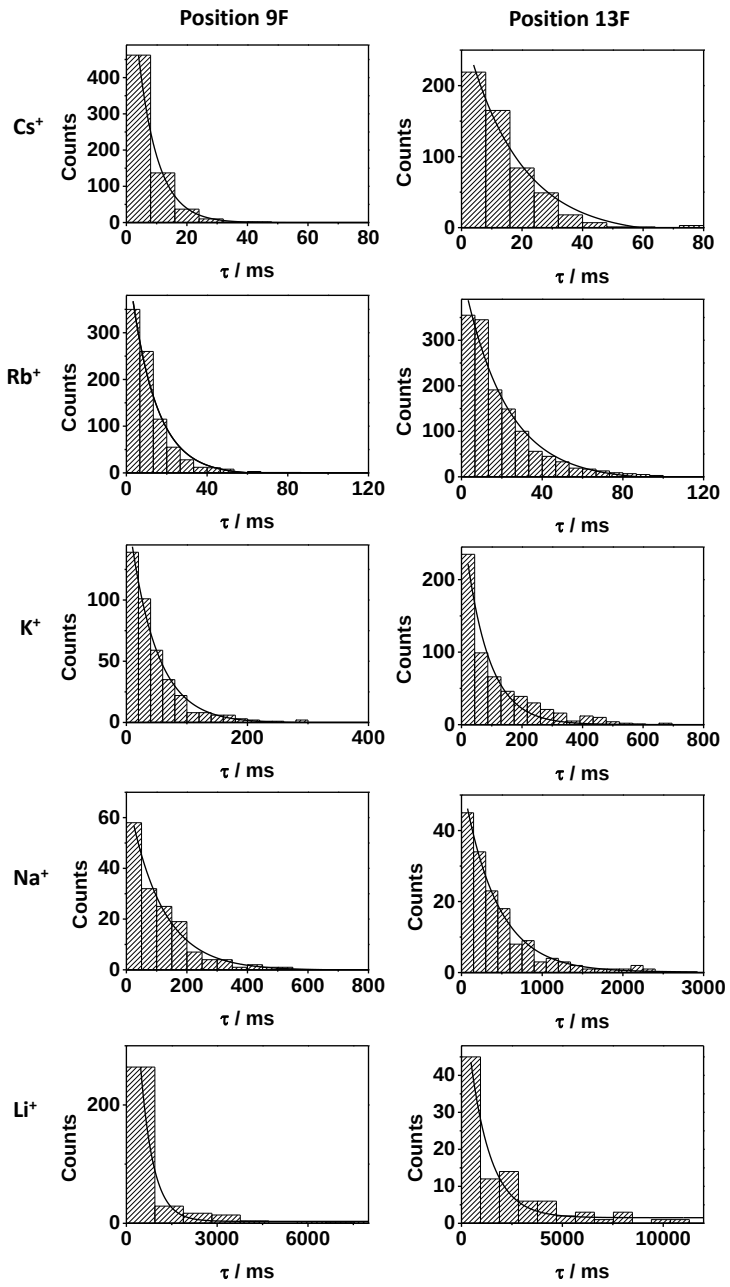

Figure S3-A. Effect of electrolyte cation on the unzipping time for the Group 1 metal ions. Data were recorded at an applied bias of 120 mV in a 10 mM phosphate buffer (pH 7.5) containing 1.00 M electrolyte. The electrolyte anion was Cl^- in all experiments.

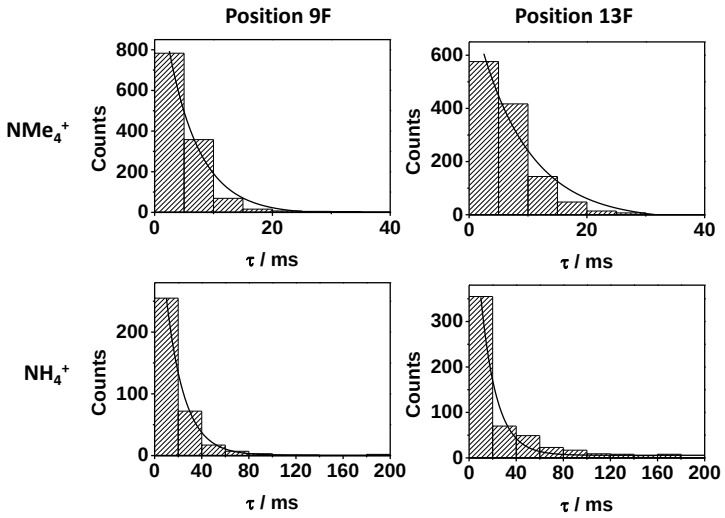

Figure S3-B. Effect of electrolyte cation on unzipping time for NMe_4^+ and NH_4^+. Data were recorded at an applied bias of 120 mV in a 10 mM phosphate buffer (pH 7.5) containing 1.00 M electrolyte. The electrolyte anion was Cl^- in all experiments.

TABLE S1. Melting temperatures (T_m) and unzipping times (τ) for duplexes 5'-TGGAGCTG**F**TGGCGTAG and 5'-TGGAGCTGCTGG**F**GTAG (bound to the complementary sequence 5'-CTACGCCAGCAGCTCCA), where the furan is positioned at the latch and outside of the latch during residence in αHL, respectively. All electrolytes contained Cl^- as the anion.

Cation	5'-TGGAGCTG**F**TGGCGTAG ACCTCGACGACCGCATC-5'		5'TGGAGCTGCTGG**F**GTAG ACCTCGACGACCGCATC-5'	
	T_m / °C	τ / ms	T_m / °C	τ / ms
Li^+	64.3 ± 0.9	292 ± 23	66.8 ± 0.8	714 ± 62
Na^+	62.7 ± 0.7	78 ± 4	65.5 ± 0.6	291 ± 16
K^+	60.7 ± 0.3	48 ± 5	64.6 ± 0.6	31 ± 3
Rb^+	61.8 ± 0.9	13 ± 3	65.0 ± 0.3	22 ± 2
Cs^+	61.7 ± .3	8 ± 1	64.3 ± 0.3	11 ± 1
NH_4^+	62.9 ± 0.6	9 ± 1	65.0 ± 0.2	10 ± 1
NMe_4^+	57.9 ± 0.3	3.7 ± 0.3	59.7 ± 0.5	6 ± 1
NEt_4^+	46.2 ± 0.5	n/a	51.6 ± 0.3	n/a

4. Full experimental details

DNA Preparation and Purification Procedures. DNA was prepared from commercially available phosphoramidites (Glen Research, Sterling, VA) by the DNA Core Facility at the University of Utah. Afterward, DNA oligomers were cleaved from the solid support and de-protected following the manufacturer's protocol, followed by purification using an ion-exchange HPLC column running a linear gradient of B from 25% to 100% over 30 min while monitoring UV absorbance at 260 nm (A = 20 mM NaPi, 1 M NaCl, pH 7 in 10% CH_3CN/90% ddH_2O, B = 10% CH_3CN/90% ddH_2O, flow rate = 3 mL/min).

Chemicals and Materials for Nanopore Measurements. All buffer solutions were prepared as 10 mM phosphate (pH 7.5), 1 mM EDTA with 1.00 M electrolyte concentration as indicated. When the electrolyte was LiCl, Tris buffer (pH 7.5) was used because of the insolubility of lithium phosphate. WT αHL was purchased from List Biological Laboratories in the monomer form of lyophilized powder and dissolved in water at 1 mg/mL. 1,2-Diphytanoyl-*sn*-glycero-3-phospho-choline (DPhPC) was dissolved in decane at 10 mg/mL and used to form the bilayer. The bilayer was supported by a glass nanopore membrane (GNM), the fabrication of which has been described previously (32). Glass nanopore membranes were modified with a 2% (v/v) (3-cyanopropyl) dimethylchlorosilane in acetonitrile to create a moderately hydrophobic surface. The DNA duplexes were annealed by mixing the 41-mer and 17-mer at a 1:2 mole ratio, followed by heating in a 90 °C water bath for 5 min and then cooling to room temperature over 3 h.

Current-Time Recordings. Current-time (*i*-*t*) recordings were performed using the low noise Nanopatch system (Electronic BioSciences, Inc., San Diego, CA) at 25°C. A voltage was applied across the GNM between two Ag/AgCl electrodes placed inside and outside of the capillary. As previously described, a lipid bilayer was deposited across the GNM orifice as indicated by a resistance increase from ~10 MΩ (associated with the open GNM) to ~100 GΩ. (32) A pressure of 60 to 80 mmHg was applied to the inside of the GNM capillary using a syringe, allowing the lipid bilayer to be functional for the protein channel reconstitution (32). Next, 0.2 μL of αHL monomer solution at 1 mg/mL was added to the *cis* side of the GNM (a volume of 350 μL). The duplex DNA (15 μM) was added to the solution reservoir after protein reconstitution into the lipid bilayer, which was indicated by a single jump in the current of approximately 1 pA /mV at

25 ° C. A voltage of 120 mV was applied *trans* vs. *cis*, (Ag/AgCl electrode inside the capillary vs. Ag/AgCl electrode placed in the external solution (*cis* negative).

Data Collection. Based on previous reports, *I-t* blockades that lasted longer than 5 ms were identified as DNA unzipping events. Unzipping events between 80 and 820 μS were attributed to translocation of single-stranded DNA (ssDNA). Events were extracted using QuB (version 1.5.0.31). Histograms of current and unzipping durations were generated and plotted using Origin Pro (version 9.0). Current histograms were fitted to Gaussian functions to obtain peak current values for each electrolyte, while time histograms were fitted to exponential functions.

Thermal Denaturation Studies. All thermal denaturation experiments were conducted with the truncated 17-mer duplexes (see below). By removing the poly-dT tails, the hyperchromic shift for the transition from double-stranded to single-stranded DNA was more clearly observed. First, the dsDNA was prepared by mixing the two complementary strands in a 1:1 ratio at a final concentration of 10 μM in 1.00 M MCl (where M = Li, Na, K, Cs, Rb, NH_4, NMe_4, or NEt_4), 10 mM PBS (for LiCl studies, Tris was used because of the insolubility of lithium phosphate), and 1 mM EDTA (pH 7.4), followed by heating the sample to 90 ^oC, then slowly cooling to room temperature over 3 h. Next, the samples were diluted to 1 μM dsDNA concentration in buffer, then loaded into T_m analysis cuvettes following the manufacturer's protocol and placed into a UV/vis spectrophotometer equipped with a temperature-regulated heat block. Samples were thermally equilibrated at 20 ^oC for 20 min followed by heating to 75 ^oC at a rate of 0.5 ^oC/min. As the samples were heated, absorbance readings at 260 nm were taken twice every minute. The background corrected data were plotted and the melting temperature (T_m) was determined using a two-point average analysis.

Truncated Native Duplex-
5'-TGGAGCTGCTGGCGTAG-3'
3'-ACCTCGACGACCGCATC-5'

Truncated duplex with G:F at position 9
5'-TGGAGCTG**F**TGGCGTAG-3'
3'-ACCTCGAC**G**ACCGCATC-5'

Truncated duplex with G:F at position 13

5’-TGGAGCTGCTGG**F**GTAG-3’

3’-ACCTCGACGACC**G**CATC-5’

5. Supplementary references

(1) Noskov, S. Y.; Im, W.; Roux, B. Ion Permeation through the α-Hemolysin Channel: Theoretical Studies Based on Brownian Dynamics and Poisson-Nernst-Plank Electrodiffusion Theory. *Biophys. J.* **2004,** *87*, 2299-2309.

(2) Bonthuis, D. J.; Zhang, J.; Hornblower, B.; Mathé, J.; Shklovskii, B. I.; Meller, A. Self-Energy-Limited Ion Transport in Subnanometer Channels. *Phys. Rev. Lett.* **2006,** *97*, 128104.

(3) De Biase, P. M.; Solano, C. J. F.; Markosyan, S.; Czapla, L.; Noskov, S. Y. Bromoc-D: Brownian Dynamics/Monte-Carlo Program Suite to Study Ion and DNA Permeation in Nanopores. *J. Chem. Theor. Comp.* **2012,** *8*, 2540-2551.

(4) Guy, A.; Piggot, T.; Khalid, S. Single-Stranded DNA within Nanopores: Conformational Dynamics and Implications for Sequencing; a Molecular Dynamics Simulation Study. *Biophys. J.* **2012,** *103*, 1028-1036.

(5) Markosyan, S.; De Biase, P. M.; Czapla, L.; Samoylova, O.; Singh, G.; Cuervo, J.; Tieleman, D. P.; Noskov, S. Y. Effect of Confinement on DNA, Solvent and Counterion Dynamics in a Model Biological Nanopore. *Nanoscale* **2014,** *6*, 9006-9016.

(6) Mathé, J.; Aksimentiev, A.; Nelson, D. R.; Schulten, K.; Meller, A. Orientation Discrimination of Single-Stranded DNA inside the A-Hemolysin Membrane Channel. *Proc. Natl. Acad. Sci. USA* **2005,** *102*, 12377-12382.